Journal of Molecular Spectroscopy 280 (2012) 27–33

Contents lists available at SciVerse ScienceDirect

Journal of Molecular Spectroscopy

journal homepage: www.elsevier.com/locate/jms

Rotational spectroscopy of 2-methylfuran from 8.7 to 960 GHz

Ian A. Finneran [a,1], Steven T. Shipman [a,*], Susanna L. Widicus Weaver [b]

[a] Division of Natural Sciences, New College of Florida, 5800 Bay Shore Road, Sarasota, FL 34243, United States
[b] Department of Chemistry, Emory University, 1515 Dickey Drive, Atlanta, GA 30322, United States

ARTICLE INFO

Article history:
Available online 15 June 2012

Keywords:
2-Methylfuran
Rotational spectroscopy
Chirped pulse
Forbidden c-types

ABSTRACT

The rotational spectrum of 2-methylfuran has been measured from 8.7 to 960 GHz using a chirped-pulse waveguide spectrometer to collect the centimeter-wave data and a direct absorption flow cell spectrometer to collect the millimeter- and submillimeter-wave data. Over 19,000 transitions in the vibrational ground state spectrum and over 6000 transitions in the spectrum of the first excited state of the methyl torsion were assigned. Fits were performed with both XIAM and ERHAM. Both programs successfully predicted the position and relative intensity of forbidden c-type transitions, but the fits from ERHAM had substantially lower RMS values than those from XIAM for roughly equivalent numbers of adjustable parameters.

1. Introduction

An area of rotational spectroscopy that has recently seen a resurgence of interest is the spectroscopy of molecules containing large amplitude internal motion. There are currently four main spectral fitting and prediction programs for internal rotors in common use: BELGI [1], ERHAM [2], SPFIT (with IAMCALC) [3] and XIAM [4]. All of these programs have been used to handle a variety of systems from the centimeter-wave to the submillimeter-wave regions, and a few recent examples include hydroxyacetone [5], isopropenyl acetate [6], *o*- and *m*-toluidine [7], and two isomers of the hydrofluoroether $C_4F_9OCH_3$ [8]. Many of these programs have hard-coded limits on the maximum number of lines or maximum value of *J*, but these values can be easily extended through direct editing of the publicly-available source code [9,10]. Their approaches and relative advantages and disadvantages have been discussed in a recent feature article in this journal [11]. ERHAM and XIAM are more straightforward to use than BELGI or the combination of SPFIT and IAMCALC because they rely upon molecular parameters that are easily extracted from the structure or other physical properties of the molecule of interest. However, because these programs do not use the extensive set of parameters implemented in BELGI or SPFIT/IAMCALC, they do not always provide fits with accuracies comparable to experimental resolution, especially in low-barrier cases. It is important to continue to benchmark the performance of each of these programs to find the program most suitable for a given molecule of interest.

In this study, we compare the performance of XIAM and ERHAM as applied in the spectroscopic analysis of 2-methylfuran (C_5H_6O, Fig. 1), a methyl-substituted derivative of furan. Furans are atmospherically-relevant volatile organic compounds (VOCs) with multiple sources, including biogenic emission from plants [12], biomass burning [13], and the cooking and frying of meat [14]. 2-Methylfuran in particular has been identified as a biomarker of cigarette smoking [15] and as a VOC emitted in tropical forest fires [16,17]. There are two prior microwave spectroscopic studies of this molecule, the initial measurement by Norris and Krisher [18], and a measurement of its dipole moment by Andresen and Dreizler [19]. Norris and Krisher collected the 2-methylfuran spectrum between 12 and 33 GHz in a Stark-modulated waveguide instrument and determined the V_3 barrier of the ground state to be 1190 cal/mol (416 cm^{-1}), giving a reduced barrier *s* of 32.6 ($s = 4V_3/9F$, where *F* is proportional to the inverse value of the moment of inertia of the rotor, which they fixed to a value of 3.14 amu $Å^2$). This corresponds to an intermediate barrier to methyl rotation. Norris and Krisher also assigned a few transitions to an excited vibrational state which had the same value of V_3 as the ground state. Subsequent work by Ogata and Kozima on 3-methylthiophene [20] compared the V_3 barrier of 2-methylfuran to the V_3 barriers of 3-methylthiophene, 2-methylthiophene [21], and 3-methylfuran [22]. This study found that the relative barrier heights in these compounds were correlated with the bond orders in the conjugated ring, with large differences in the bond orders of alternating bonds leading to large barrier heights for internal rotation of the methyl group.

2-Methylfuran is a methyl-rotor containing species with Ray's asymmetry parameter $\kappa = -0.67$. This has the consequence that at only modest levels of excitation, the asymmetry splitting and the internal rotor splitting become nearly equal to each other,

* Corresponding author. Fax: +1 941 487 4396.
E-mail address: shipman@ncf.edu (S.T. Shipman).
[1] Present address: Division of Chemistry and Chemical Engineering, California Institute of Technology, Pasadena, CA 91125, United States.

0022-2852/$ - see front matter © 2012 Elsevier Inc. All rights reserved.
http://dx.doi.org/10.1016/j.jms.2012.06.005

leading to level mixing. This level mixing can potentially lead to problems with consistent labeling of energy levels. Also, level mixing allows transitions that would otherwise be forbidden to appear in the spectrum, borrowing intensity from normally allowed transitions [23–25]. In the case of 2-methylfuran, this effect results in intense ^{c}R transitions, despite the fact that by symmetry this molecule has a zero value of μ_c. It is therefore interesting to see how well the internal rotor programs can handle issues of this type, particularly at the high values of J and K_a associated with submillimeter-wave spectra.

In this work, we report on the rotational spectrum of 2-methylfuran, collected over a broad frequency range from 8.7 to 960 GHz. We used a room-temperature chirped-pulse Fourier transform microwave spectrometer to collect the cm-wave spectrum and a direct absorption flow cell spectrometer to collect the mm- and submm-wave data. We have assigned the ground vibrational state spectrum of this molecule up to high values of J and K_a using XIAM and ERHAM. Here we present the results of the spectroscopic study, the resultant analysis, and a discussion of discrepancies between the fits from these two programs. Additionally, we report the assigned rotational spectrum for the first excited state of the methyl torsional mode in this molecule.

2. Experimental

The room temperature chirped-pulse microwave spectrometer used to collect the cm-wave spectrum of 2-methylfuran from 8.7 to 18.3 GHz has been described previously [26]; its design is based on the chirped-pulse molecular-beam instrument previously described by Pate and co-workers [27]. The sample was introduced into a 10-m coiled static-cell waveguide (WRD-750) at a pressure of ~11 mTorr, and cooled to 0 °C by immersing the waveguide in an ice water bath. The sample of 2-methylfuran (99%) was acquired from Sigma–Aldrich, and purified with several freeze–pump–thaw cycles. The microwave spectrum of 2-methylfuran was collected in two bands, 8.7–13.5 GHz and 13.5–18.3 GHz. A chirped pulse from 0.1 to 4.9 GHz was generated with an arbitrary waveform generator (AWG7101, Tektronix) and shifted to either of the two operating bands using a mixer (DM0520LW1, Miteq) and a local oscillator (PLO-4000, Microwave Dynamics) with a frequency of either 13.6 or 18.4 GHz. The frequency-shifted pulses were amplified by a 10 W solid-state amplifier (L0618-40-T526, Microwave Power) and broadcast into the waveguide, where they polarized the molecular sample. The subsequent free induction decay (FID) was amplified with a high-gain, low-noise amplifier (AMF-5F-08001800-14-10P-1, Miteq), shifted down to 0.1–4.9 GHz with a second mixer (DM0520LW1, Miteq) and the same local oscillator, and detected by a high-speed digital oscilloscope (TDS6154C, Tektronix). The FID was collected for 4 μs and a Fourier transform was performed to yield the frequency domain spectrum.

Spectra of 2-methylfuran above 75 GHz were collected using a single-pass, direct-absorption flow cell spectrometer at Emory University, which has been described previously [28]. Source radiation was generated by an Agilent E8257D microwave synthesizer coupled to frequency multiplier chains from Virginia Diodes, Inc. The detector used was a QMC Instruments QFI/2BI InSb hot electron bolometer. The synthesizer output was frequency modulated at 15 kHz using the internal reference of the microwave synthesizer, and the bolometer signal was detected by a Stanford Research SR830 lock-in amplifier using 2f detection. The 2-methylfuran sample was introduced into the 2.1-m flow cell using a needle valve, and a stable pressure of 35 mTorr was maintained by a throttled vacuum pump throughout the data collection. The spectrum was acquired with a resolution of 100 kHz. At low frequencies, this step size is the dominant source of frequency uncertainty in the spectral lines. At higher frequencies, Doppler broadening dominates the linewidths and hence the frequency uncertainty. For simplicity, all frequencies were assigned a conservative estimated uncertainty of 150 kHz. Spectra were obtained in the following spectral ranges: 75–125 GHz, 130–450 GHz, 460–650 GHz, 700–732 GHz, 760–969 GHz.

A variety of software was used throughout this work. All *ab initio* calculations were performed with Gaussian 03, Rev. E01 [29]. Spectral visualizations and assignments were made with AABS [30], and both ERHAM [2] and XIAM [4] were used to fit the spectra. The rotational spectroscopy programs and several utilities are available for download from the PROSPE website [9,10], many in both source code and executable formats. Due to the large number of lines measured and the high J values to which the fits were extended, modifications were made to both the XIAM and ERHAM source codes to handle the full data sets. These modifications primarily involved changing maximum array dimensions and recompiling. Additionally, a number of Python scripts were written to convert line lists and predictions from one format to another and to enable straightforward operation with AABS. These scripts are available upon request.

3. Results

3.1. Overview

Based on previous far-IR spectral studies [31] and *ab initio* calculations, it is known that 2-methylfuran has three normal modes with frequencies below 400 cm^{-1} – the methyl torsion (158 cm^{-1}), an out-of-plane bend of the methyl group (237 cm^{-1}), and an in-plane bend of the methyl group (339 cm^{-1}). Transitions from each of these states as well as their low-lying overtones or combination bands may be present in the observed spectra, which were collected at 273 K (8.7–18.3 GHz data) and 298 K (75–960 GHz data).

The rotational spectrum of 2-methylfuran has several characteristic features (Fig. 2). First, the presence of a methyl rotor with a modest V_3 barrier leads to A–E splittings on the order of MHz for every rotational transition in the ground state. Second, 2-methylfuran has non-zero μ_a and μ_b components of the dipole moment, which allows for the presence of intense spectral features corresponding to quartets comprised of pairs of ^{a}R and ^{b}R transitions at high values of J and low values of K_a. As K_a increases, the spacing between these transitions also increases, leading to characteristic patterns in the spectrum. Finally, the internal rotor leads to the presence of strong c-type transitions, despite the lack of a permanent dipole moment component along the c-axis by symmetry. This occurs in the E-state when the asymmetry splitting is similar in magnitude to the A–E splitting, and these transitions acquire

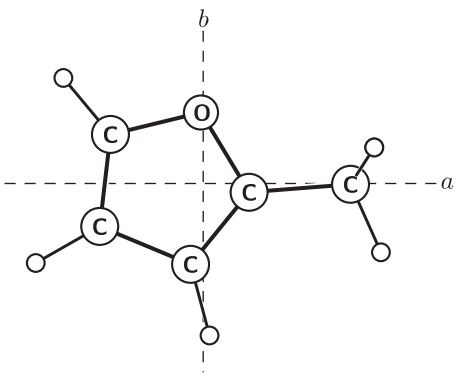

Fig. 1. 2-Methylfuran in the principal axis system. Only the hydrogen atoms on the methyl rotor lie outside of the *ab*-plane.

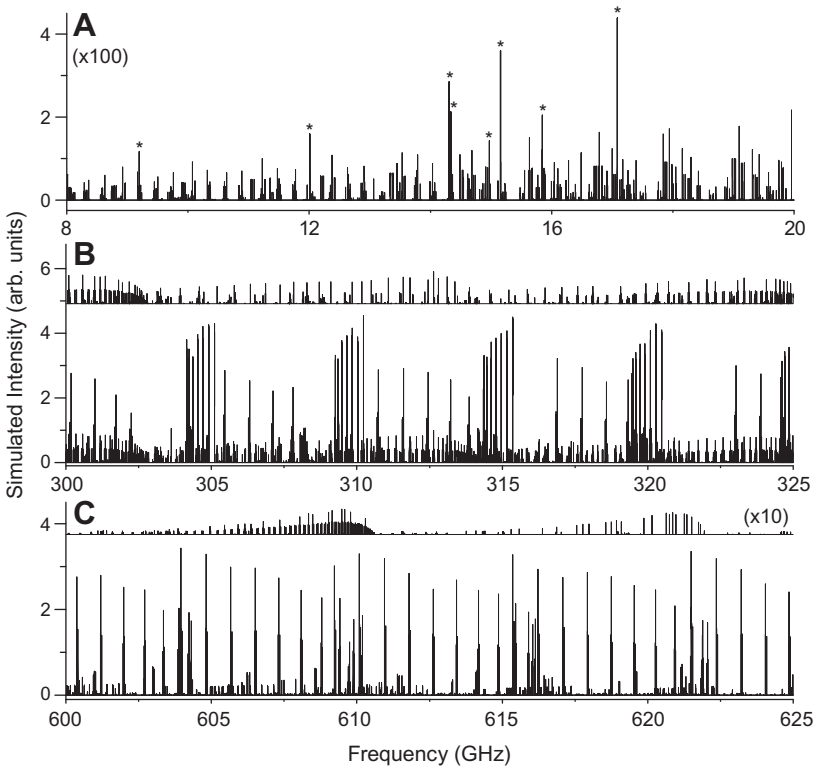

Fig. 2. Simulated spectrum for the 2-methylfuran ground state from 8 to 20 GHz (A), 300–325 GHz (B), and 600–625 GHz (C). (A) The strong transitions in this frequency region are ^{b}Q transitions (indicated with an asterisk). The dense collection of weaker transitions is comprised of primarily ^{b}R and ^{b}P transitions and "forbidden" ^{c}R and ^{c}P transitions (see text for details). Intensities have been multiplied by a factor of 100 to put this panel on approximately the same scale as panels B and C. (B) In this frequency range, the dominant peaks are the tight clusters of strong ^{a}R and ^{b}R transitions, and the weaker, sparser peaks are due to ^{b}R and "forbidden" ^{c}R transitions. There are also dense but weak ^{b}Q transitions throughout this frequency range; these have been offset for clarity. (C) In this frequency range, the ^{b}R and "forbidden" ^{c}R transitions are now dominant. The weak ^{b}Q transitions have been offset and scaled by a factor of 10 for clarity.

intensity by borrowing it from allowed b-type transitions [23–25]. The asymmetry splitting decreases for symmetric molecules (as $|\kappa|$ approaches 1) and for large K_a in near-prolate molecules. The previous studies of 2-methylfuran [18,19] did not extend analysis to sufficiently high values of K_a to observe forbidden transitions.

3.2. Ground state spectrum

Starting with the previous ground state constants [18], the cm-wave spectrum was assigned by the usual method of incrementally adding line assignments to the fit and gradually increasing J and K_a in stages. There are a handful of strong ^{b}Q transitions in this region of the spectrum. Beneath these is a dense forest of ^{b}R, ^{b}P, ^{c}R, and ^{c}P transitions (Fig. 2A). Using only the cm-wave data, we were able to assign the ground state spectrum up to $J = 71$ and $K_a = 37$ (Fig. 3). Due to the 412.8 cm^{-1} value of V_3, typical A–E splittings in the ground state were on the order of a few MHz; this is large enough for these transitions to be resolved, but small enough that the A–E pairs were easily identified (Fig. 3C).

The cm-wave constants were then used as a starting point to assign the mm- and submm-wave spectrum from the Emory spectrometer (Fig. 4). Between 75 and 450 GHz, the strong ^{a}R and ^{b}R transitions were easily picked out of the spectrum and assigned. These transitions had sufficient signal-to-noise ratios to enable confident assignments up to $J = 120$. Above 400 GHz, ^{b}R and ^{c}R transitions contribute the majority of the strong peaks; these assignments were also straightforward due to the quality of the prediction. Finally, once these R-branch transitions were assigned, the quality of the fit and prediction were sufficient to assign the dense but weak spectrum of ^{b}Q transitions.

Due to the extensive nature of the spectral coverage, combination loops could be used to aid assignment of new transitions and to identify potentially incorrect assignments. Due to their weak intensities, the transitions with the least certain assignments were the ^{b}Q transitions. A script was written to go through the list of assigned transitions and generate all possible three- and four-level combination loops involving one or more ^{b}Q transitions. Loops containing only one unidentified transition provided frequencies for potential assignments, and loops with all transitions identified were used to assess the quality of the assignments. If a loop summed to a value greater than 0.5 MHz, then all transitions in the loop were removed from the list of assigned transitions and not included in the final analysis.

Both XIAM and ERHAM were used to assign the ground vibrational state spectrum, and the final fit parameters from each program are summarized in Table 1. XIAM does not report the standard deviation of the fit, and so the reduced root mean squared (RMS) deviation is used to compare the relative fit qualities. For the large number of transitions in the present fits, the difference between the reduced RMS deviation and reduced standard deviation is not significant (0.718 for the reduced RMS deviation and 0.719 for the reduced standard deviation from the ground state fit in ERHAM). The parameters used represent the minimal set within each program where every parameter is determined to better than 10%. It is possible to further reduce the fit RMS by a few percent by adding additional parameters to the fit; however, the value of this exercise is questionable, as extra parameters with large relative uncertainties do not provide much additional physical insight. Discrepancies between the results from these two programs will be discussed below. Any transition with an observed–calculated residual greater than five times the uncertainty was not included in the final fit. An appreciable fraction of the assigned lines were blended lines involving two or four transitions with predicted frequencies that differed by less than 1 kHz. Table 1 reports the num-

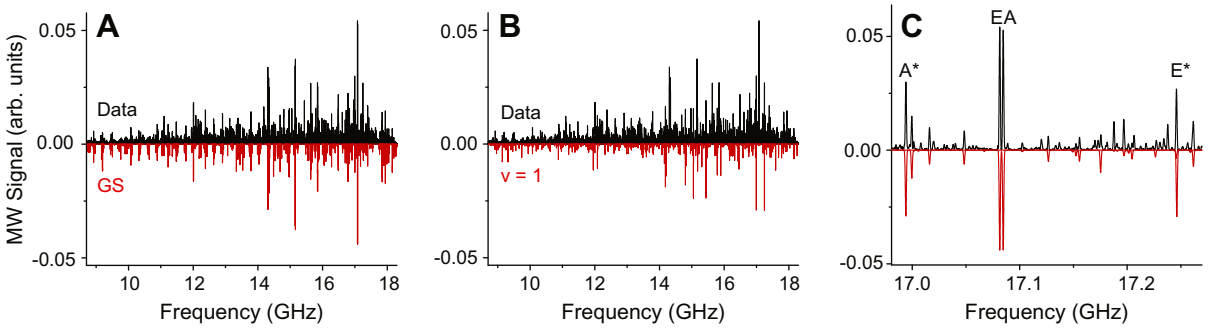

Fig. 3. Experimental and simulated cm-wave spectra for 2-methylfuran ground and excited torsional state. In all panels, the experimental data is positive-going and the simulated data is negative-going. The intensity scale in these panels is the same as the (unscaled) intensity axis in panel A of Fig. 2. In both panels B and C, the simulated data for the excited state was scaled by a factor of 2/3 relative to the ground state to match the experimental data. (A) 2-methylfuran experimental spectrum versus the ground state simulated spectrum. (B) 2-methylfuran experimental spectrum versus the excited torsional state simulated spectrum. (C) Inset showing an expanded view of the data and simulated spectra of both the ground and excited states. The A–E splitting in the torsionally excited state (251.8 MHz, transitions marked with asterisks) is substantially larger than that of the ground state (3.2 MHz) for the 7_{25}–7_{16} transition.

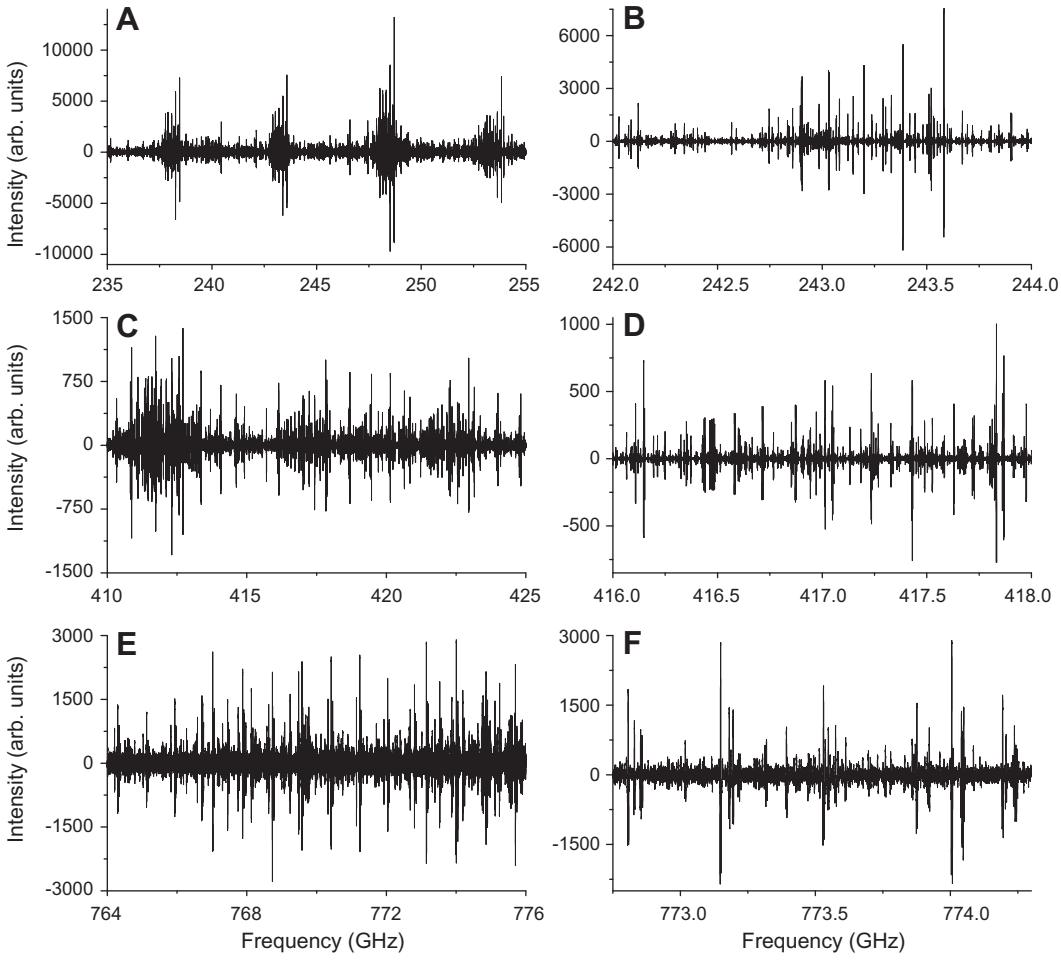

Fig. 4. Representative portions of the mm-wave and submm-wave spectra collected on the direct absorption flow cell spectrometer. Panels in the right column (B, D, and F) are expanded views of panels in the left column (A, C, and E). In panels A and B, showing data near 245 GHz, the intense peaks are due to low-K_a ^aR and ^bR transitions. Panels C and D show data near 420 GHz, where ^aR, ^bR, and ^cR transitions are intense. In this region, low-K_a ^aR and ^bR transitions appear in tight clusters (peak spacings on the order of 100 MHz) and low-K_c ^bR and ^cR transitions are more sparse (peak spacings on the order 1 GHz). Panels E and F show data near 770 GHz, where virtually all of the intense peaks are due to low-K_c ^bR and ^cR transitions.

ber of distinct frequencies in the fit, with the total number of transitions indicated in the footnote. More lines were included in the ERHAM analysis than in the XIAM analysis because XIAM does not properly weight blended transitions. Therefore, only unblended transitions were included in the XIAM fit.

3.3. Torsionally excited state spectrum

Due to both its reduced intensity and its substantially greater A–E splitting, the initial assignment of the first excited state of the methyl torsional mode (*ab initio* frequency of 158 cm^{-1}) was

Table 1
Molecular parameters for the ground vibrational state of 2-methylfuran. 1-σ uncertainties are listed in parentheses in the units of the last significant digit.

	Calculated[a]		XIAM		ERHAM
A (MHz)	8756.7754		8792.22489(33)		8791.54486(12)
B (MHz)	3537.1200		3542.64071(20)		3543.321804(46)
C (MHz)	2559.8639		2565.560151(38)		2565.603243(36)
Δ_J (kHz)	0.25545138		1.539273(68)		0.2645388(58)
Δ_{JK} (kHz)	1.3677974		−2.41323(31)		1.408544(66)
Δ_K (kHz)	1.0616181		0.99269(31)		1.000997(83)
δ_J (kHz)	0.070719708		0.564919(32)		0.0724207(24)
δ_K (kHz)	0.60351449		−0.46139(17)		0.687123(86)
		Φ_{JK} (mHz)	−0.669(45)		−0.6653(83)
		Φ_{KJ} (mHz)	0.568(50)		[0.0]
		Φ_K (mHz)	[0.0]		1.882(20)
		φ_{JK} (mHz)	−0.502(29)		[0.0]
V_3 (cm^{-1})	368.8[b]		412.873(74)	ε_1 (MHz)	−119.459(11)
		Δ_{Jm} (MHz)	−0.0950(30)	$B020_1$[e] (kHz)	1.051(29)
		Δ_{Km} (MHz)	0.2333(73)	$B220_1$ (Hz)	−0.1781(88)
		δ_m (MHz)	0.0406(27)	$B202_1$ (Hz)	0.0133(11)
				$B004_1$ (Hz)	−0.03557(84)
				$B600_1$ (mHz)	0.00603(23)
		ρ	0.0549511(44)		0.0550406(14)
$<(i, x)$	4.48		3.30(13)	β (°)	1.908(13)
$<(i, y)$	85.52		86.70(13)		
$<(i, z)$	90.00		90.009(18)		
		J max	95		120
		K_a max	53		54
		N	8006[d]		11793[f]
		σ_{fit} (MHz)	0.263		0.108
		σ_w[c]	1.754		0.718

[a] From an *ab initio* calculation evaluated at the MP2/6-311++G(d,p) level using Gaussian 03 [29].
[b] Fit to a relaxed potential energy scan at the same level of theory.
[c] Root mean square deviation of a weighted fit.
[d] Only unblended transitions were used in the fit.
[e] Tunneling parameters in the effective Hamiltonian, following the labeling scheme used in Refs. [2,33].
[f] This is the number of distinct frequencies used in the fit. Due to extensive blending caused by the near-degeneracy of many transitions, this represents a total of 19,143 transitions.

performed using the high-frequency spectra from the Emory spectrometer rather than the cm-wave spectra from the New College spectrometer. The strong ^{a}R and ^{b}R transitions were used to establish the fit, after which a few ^{b}Q transitions in relatively sparse regions of the spectrum could be assigned. These were then used in conjunction with the combination loops described above to greatly extend the number of lines in the fit. Unfortunately, it was not possible to extend the fit to $K_a > 15$, possibly due to a perturbation with the out-of-plane bending mode (*ab initio* frequency of 237 cm^{-1}). Because of this relatively low maximum K_a value, no assignments could be made for any forbidden c-type transitions affiliated with this state. The analysis for this state therefore included only ^{a}R, ^{b}R, and ^{b}Q transitions.

A fit for this state up to $K_a = 15$ using ERHAM is presented in Table 2. As for the ground state, transitions with observed frequencies differing from their predicted frequencies by more than five times the uncertainty were discarded, as were transitions that were part of closed combination loops summing to a frequency greater than 0.5 MHz.

3.4. Other vibrationally excited states

The previous work by Norris and Krisher assigned 14 transitions between 20 and 30 GHz to a vibrationally excited state with A–E splittings similar to those of the ground state [18]. They attribute this to the first excited state of a ring-puckering mode. However, based on the vibrational frequencies predicted in the *ab initio* calculations, this excited state is more likely an out-of-plane bend (237 versus 603 cm^{-1}). Despite an extensive search, no lines could be assigned to this vibrationally-excited state. However, there are a number of unassigned lines remaining in the present data set. Further, no spectra were obtained in the 20–30 GHz frequency range, precluding verification of the previously observed lines. It should be noted that two of the 14 reported lines (20173.16 MHz and 26221.47 MHz) are within 150 kHz of relatively strong predicted transitions for the ground state and first excited state of the methyl torsional mode, and could easily have been misassignments. Future work will focus on collecting the 2-methylfuran spectrum between 18 and 26.5 GHz using a newly-constructed room-temperature spectrometer; this will allow several of the previously assigned transitions for this state to be remeasured, and possibly enable extension of the previous fit of this excited state to substantially higher J and K_a values.

4. Discussion

Both XIAM and ERHAM (modified to handle the large data set) have been used to fit the ground state spectrum of 2-methylfuran. These two programs have been compared in other work [6,8,32–34], and it is generally the case that ERHAM yields higher-quality fits at the cost of straightforward comparison to the results of *ab initio* calculations. In particular, it is not possible to directly fit V_3 in ERHAM, while this is a fit parameter in XIAM. The primary shortcoming of XIAM is a lack of high-order distortion constants for the internal rotation part of the Hamiltonian. Both programs have a similar ease-of-use once the user becomes familiar with the input and output file formats.

In the present case, the assignment process began with XIAM due to its ability to directly map the starting fit parameters (A, B, C, quartic distortion constants, V_3, and the rotor axis angles) to the output of *ab initio* optimizations and relaxed potential energy scans. During the ground state assignment process, it was noticed both that transitions involving levels with K_a near 11 had unusually high residuals (see Fig. 5) and that the quartic distortion con-

Table 2
Molecular parameters for the first excited torsional state of 2-methylfuran. 1-σ uncertainties are listed in parentheses in the units of the last significant digit.

	ERHAM
A (MHz)	8790.0922(18)
B (MHz)	3540.94203(22)
C (MHz)	2564.946450(65)
Δ_J (kHz)	0.268855(50)
Δ_{JK} (kHz)	1.8300(31)
Δ_K (kHz)	−1.947(21)
δ_J (kHz)	0.074930(24)
δ_K (kHz)	0.6824(14)
Φ_{JK} (mHz)	−2.852(63)
ϕ_K (mHz)	−7.01(64)
ε_1 (MHz)	3781.55(72)
$B020_1$ (MHz)	−0.3910(35)
$B200_1$ (MHz)	0.017418(49)
$B220_1$ (kHz)	−0.1102(27)
$B022_1$ (kHz)	−0.0523(14)
$B202_1$ (Hz)	−5.335(12)
$B040_1$ (kHz)	0.806(10)
$B400_1$ (kHz)	−0.010640(23)
$B240_1$ (Hz)	0.0785(35)
$B042_1$ (Hz)	0.0523(25)
$B420_1$ (mHz)	1.354(61)
ρ	0.0554463(90)
β (°)	2.1785(31)
J max	114
K_a max	15
N	2580[b]
σ_{fit} (MHz)	0.113
σ_w[a]	0.753

[a] Root mean square deviation of a weighted fit.
[b] This is the number of distinct frequencies used in the fit. Due to extensive blending caused by the near-degeneracy of many transitions, this represents a total of 6128 transitions.

stants were substantially different from the *ab initio* predictions (see Table 1). One possibility was that this was the result of perturbations from an excited vibrational state; however, this seemed unlikely, as the next vibrationally-excited state, the methyl torsion, is much higher in energy (158 cm^{-1}). Perturbations of the ground state spectrum near these K_a values have been seen in the acrylonitrile spectrum [35]. However, in that case the A rotational constant was substantially larger than in the present case. Additionally, the difficulties in the present study were appearing at rather low values of the J quantum number, i.e. as early as $J = 30$, rather than becoming prominent near $J = 80$ or higher as in acrylonitrile.

Thorough examination of the fit statistics and predicted lower state energies revealed that these problems were independent of the A–E splittings predicted by XIAM. Switching to ERHAM immediately removed this problem (see Fig. 5), and further led to a substantially-reduced RMS uncertainty with only one additional adjustable parameter. It appears that the omission of internal rotor centrifugal distortion parameters in XIAM was forcing the rigid rotor distortion constants to compensate, leading to a fit of an overall lower quality. Despite this problem, both ERHAM and XIAM provide successful predictions of the forbidden c-type transitions, with roughly correct relative intensities.

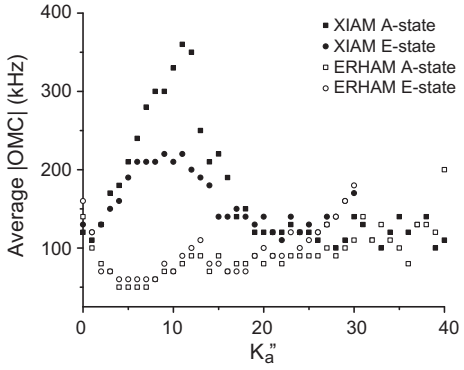

Fig. 5. Comparison of XIAM and ERHAM fit quality for the 2-methylfuran ground state. The average absolute value of the observed minus calculated frequency residual is plotted as a function of K_a'' for transitions with J'' ranging from 15 to 100. Each point on the plot is the average of more than 100 transitions. The lack of sufficient distortion constants in XIAM leads to severe fit difficulties for transitions involving K_a'' values near 11.

There are apparent anomalies in the fits of both states with ERHAM, despite the success of the predictions. In both the ground and excited state fits, tunneling parameters were used that correspond to sextic distortion constants that were held fixed at zero. These are $B600_1$ in the ground state (corresponding to Φ_J) and $B240_1$ in the excited state (corresponding to Φ_{KJ}). When added, the sextic distortion constants cannot be well-determined and do not significantly improve the quality of the fit, and removal of their associated tunneling parameters harms the fit quality, increasing the reduced RMS deviation by roughly 10%. Additionally, the $B004_1$ constant has been included in the ground state fit, despite the fact that this is a tunneling parameter associated with the S-reduction Hamiltonian. Inclusion of this parameter decidedly helps the fit, again by roughly 10%, but there is not an obvious reason why this should be the case.

Although it has been previously noted that ERHAM can more accurately fit the spectra of molecules with internal rotors than XIAM, the extent of XIAM's failure in this case is surprising. While it seems clear that ERHAM's tunneling parameters allow it to succeed where XIAM does not, the tunneling parameters from ERHAM for the 2-methylfuran ground state do not have particularly large magnitudes (Table 1). In fact, the 2-methylfuran ground state tunneling parameters are smaller by factors of 10 or more than those reported for pyruvonitrile [32] and pyruvic acid [33]. However, the difference in fit quality between XIAM and ERHAM is much more pronounced in the present case. The discrepancy between the two programs was much worse in the first excited state of the methyl torsional mode than in the ground state, because XIAM was unable to fit the excited state data set to an RMS better than 16 MHz, in comparison to ERHAM's fit RMS of 113 kHz. It is apparent from comparing the fits from ERHAM in Tables 1 and 2 that many additional tunneling parameters were needed to properly fit the rotational spectrum of the vibrationally-excited state, and the tunneling parameters themselves are factors of 50–1000 times larger than in the ground state. Given these results, it is not surprising that XIAM provided a less accurate fit for the torsionally excited state than for the ground state.

5. Conclusions

The rotational spectrum of 2-methylfuran was collected from 8.7 to 960 GHz using a centimeter-wave chirped-pulse Fourier transform microwave spectrometer and a millimeter- and submillimeter-wave direct absorption flow cell spectrometer. Over 19,000 transitions in the ground state spectrum were fit to an RMS of 108 kHz, and over 6000 transitions in the spectrum of the first torsionally excited state were fit to an RMS of 113 kHz. Fits performed with ERHAM had significantly lower RMS values than those performed with XIAM, presumably due to XIAM's limited set of internal rotor distortion parameters.

Acknowledgments

I.A.F. and S.T.S. acknowledge the Research Corporation for Science Advancement and the Donors of the American Chemical Society Petroleum Research Fund for support of this research. S.T.S.

also acknowledges New College of Florida for start-up funding. S.L.W.W. acknowledges support for spectrometer development from NASA award number NNX11AI07G, and start-up support from Emory University.

Appendix A. Supplementary data

Supplementary data for this article are available on ScienceDirect (www.sciencedirect.com) and as part of the Ohio State University Molecular Spectroscopy Archives (http://library.osu.edu/sites/msa/jmsa_hp.htm).

Supplementary data associated with this article can be found, in the online version, at http://dx.doi.org/10.1016/j.jms.2012.06.005.

References

[1] J.T. Hougen, I. Kleiner, M. Godefroid, J. Mol. Spectrosc. 163 (1994) 559.
[2] P. Groner, J. Chem. Phys. 107 (1997) 4483.
[3] J.M. Pickett, J. Mol. Spectrosc. 148 (1991) 371.
[4] H. Hartwig, H. Dreizler, Z. Naturforsch. 51a (1996) 923.
[5] R. Braakman, B.J. Drouin, S.L. Widicus Weaver, G.A. Blake, J. Mol. Spectrosc. 264 (2010) 43.
[6] W. Stahl, H.V.L. Nguyen, J. Mol. Spectrosc. 264 (2010) 120.
[7] R.G. Bird, D.W. Pratt, J. Mol. Spectrosc. 266 (2011) 81.
[8] G.S. Grubbs II, S.A. Cooke, J. Phys. Chem. A 115 (2011) 1086.
[9] Z. Kisiel, *PROSPE – Programs for Rotational Spectroscopy*, <http://info.ifpan.edu.pl/~kisiel/prospe.htm>.
[10] Z. Kisiel, in: J. Demaison et al. (Eds.), Spectroscopy from Space, Kluwer Academic Publishers, Dordrecht, 2001, pp. 91–106.
[11] I. Kleiner, J. Mol. Spectrosc. 260 (2010) 1.
[12] V.A. Isidorov, I.G. Zenkevich, B.V. Ioffe, Atmos. Environ. 19 (1985) 1.
[13] M.O. Andreae, P. Merlet, Global Biogeochem. Cycles 15 (2001) 955.
[14] W.F. Rogge, L.M. Hildermann, M.A. Mazurek, G.R. Cass, B.R.T. Simoneit, Environ. Sci. Technol. 25 (1991) 1112.
[15] J.J.B.N. Van Berkel, J.W. Dallinga, G.M. Möller, R.W.L. Godschalk, E. Moonen, E.F.M. Wouters, F.J. Van Schooten, J. Chromatogr. B 861 (2008) 101.
[16] R.J. Yokelson, T. Karl, P. Artaxo, D.R. Blake, T.J. Christian, D.W.T. Griffith, A. Guenther, W.M. Hao, Atmos. Chem. Phys. 7 (2007) 5175.
[17] T.G. Karl, T.J. Christian, R.J. Yokelson, P. Artaxo, W.M. Hao, A. Guenther, Atmos. Chem. Phys. 7 (2007) 5883.
[18] W.G. Norris, L.C. Krisher, J. Chem. Phys. 51 (1969) 403.
[19] U. Andresen, H. Dreizler, Z. Naturforsch. A 25 (1970) 570.
[20] T. Ogata, K. Kozima, J. Mol. Spectrosc. 42 (1972) 38.
[21] N.M. Pozdeev, R.G. Latypova, L.N. Gunderova, J. Struct. Chem. 17 (1976) 313.
[22] T. Ogata, K. Kozima, Bull. Chem. Soc. Jpn. 44 (1971) 2344.
[23] R.C. Woods, J. Mol. Spectrosc. 21 (1966) 4.
[24] G.M. Plummer, E. Herbst, F.C. De Lucia, Astrophys. J. 318 (1987) 873.
[25] D.R. Herschbach, J.D. Swalen, J. Chem. Phys. 29 (1958) 761.
[26] B. Reinhold, I.A. Finneran, S.T. Shipman, J. Mol. Spectrosc. 270 (2011) 89.
[27] G.G. Brown, B.C. Dian, K.O. Douglass, S.M. Geyer, S.T. Shipman, B.H. Pate, Rev. Sci. Inst. 79 (2008) 053103.
[28] P.B. Carroll, B.J. Drouin, S.L. Widicus Weaver, ApJ 723 (2010) 845.
[29] M.J. Frisch, G.W. Trucks, H.B. Schlegel, G.E. Scuseria, M.A. Robb, J.R. Cheeseman, J.A. Montgomery, Jr., T. Vreven, K.N. Kudin, J.C. Burant, J.M. Millam, S.S. Iyengar, J. Tomasi, V. Barone, B. Mennucci, M. Cossi, G. Scalmani, N. Rega, G.A. Petersson, H. Nakatsuji, M. Hada, M. Ehara, K. Toyota, R. Fukuda, J. Hasegawa, M. Ishida, T. Nakajima, Y. Honda, O. Kitao, H. Nakai, M. Klene, X. Li, J.E. Knox, H.P. Hratchian, J.B. Cross, V. Bakken, C. Adamo, J. Jaramillo, R. Gomperts, R.E. Stratmann, O. Yazyev, A.J. Austin, R. Cammi, C. Pomelli, J.W. Ochterski, P.Y. Ayala, K. Morokuma, G.A. Voth, P. Salvador, J.J. Dannenberg, V.G. Zakrzewski, S. Dapprich, A.D. Daniels, M.C. Strain, O. Farkas, D.K. Malick, A.D. Rabuck, K. Raghavachari, J.B. Foresman, J.V. Ortiz, Q. Cui, A.G. Baboul, S. Clifford, J. Cioslowski, B.B. Stefanov, G. Liu, A. Liashenko, P. Piskorz, I. Komaromi, R.L. Martin, D.J. Fox, T. Keith, M.A. Al-Laham, C.Y. Peng, A. Nanayakkara, M. Challacombe, P.M.W. Gill, B. Johnson, W. Chen, M.W. Wong, C. Gonzalez, J.A. Pople, Gaussian 03, Revision E.01, Gaussian, Inc., Wallingford CT, 2004.
[30] Z. Kisiel, L. Pszczółkowski, I.R. Medvedev, M. Winnewisser, F.C. De Lucia, E.C. Herbst, J. Mol. Spectrosc. 233 (2005) 231.
[31] D.W. Scott, J. Mol. Spectrosc. 37 (1971) 77.
[32] A. Kraśnicki, Pszczółkowski, Z. Kisiel, J. Mol. Spectrosc. 260 (2010) 57.
[33] Z. Kisiel, L. Pszczółkowski, E. Białkowska-Jaworska, S.B. Charnley, J. Mol. Spectrosc. 241 (2007) 220.
[34] F.J. Lovas, D.F. Plusquellic, S.L. Widicus Weaver, B.A. McGuire, G.A. Blake, J. Mol. Spectrosc. 264 (2010) 10.
[35] Z. Kisiel, L. Pszczółkowski, B.J. Drouin, C.S. Brauer, S. Yu, J.C. Pearson, J. Mol. Spectrosc. 258 (2009) 26.